Front. Struct. Civ. Eng. 2024, 18(7): 1066–1083
https://doi.org/10.1007/s11709-024-1084-0

RESEARCH ARTICLE

Design parameter optimization method for a prestressed steel structure driven by multi-factor coupling

Guo-Liang SHI[a,b], Zhan-Sheng LIU[a,b*], De-Chun LU[a,b], Qing-Wen ZHANG[a,b], Majid DEZHKAM[a,b], Ze-Qiang WANG[c]

[a] *Faculty of Architecture, Civil and Transportation Engineering, Beijing University of Technology, Beijing 100124, China*
[b] *The Key Laboratory of Urban Security and Disaster Engineering of the Ministry of Education, Beijing University of Technology, Beijing 100124, China*
[c] *Beijing Building Construction Research Institute Co., Ltd., Beijing 100039, China*
[*] *Corresponding author. E-mail: liuzhansheng@bjut.edu.cn*

ABSTRACT To achieve efficient structural design, it is crucial to reduce the cost of materials while ensuring structural safety. This study proposes an optimization method for design parameters (DPs) in a prestressed steel structure driven by multi-factor coupling. To accomplish this, a numerical proxy model of prestressed steel structures is established with integration of DPs and mechanical parameters (MPs). A data association-parameter analysis-optimization selection system is established. A correlation between DPs and MPs is established using a back propagation (BP) neural network. This correlation provides samples for parameter analysis and optimization selection. MPs are used to characterize the safety of the structure. Based on the safety grade analysis, the key DPs that affect the mechanical properties of the structure are obtained. A mapping function is created to match the MPs and the key DPs. The optimal structural DPs are obtained by setting structural materials as the optimization objective and safety energy as the constraint condition. The theoretical model is applied to an 80-m-span gymnasium and verified with a scale test physical model. The MPs obtained using the proposed method are in good agreement with the experimental results. Compared with the traditional design method, the design cycle can be shortened by more than 90%. Driven by the optimal selection method, a saving of more than 20% can be achieved through reduction of structural material quantities. Moreover, the cross-sectional dimensions of radial cables have a substantial influence on vertical displacement. The initial tension and cross-sectional size of the upper radial cable exhibit the most pronounced impact on the stress distribution in that cable. The initial tension and cross-sectional size of the lower radial cable hold the greatest sway over the stress distribution in that cable.

KEYWORDS structure design, association relationship, performance analysis, optimum selection, experimental verification

1 Introduction

Challenges in prestressed steel structure design include intricate and diverse design variables and a substantial solution scale [1]. In the process of design, it is crucial to consider not only the principles of mechanical behavior (e.g., structural strength and stability) but also to optimize structure.

Article history: Received Aug 30, 2023; Accepted Nov 9, 2023

1.1 Design method of prestressed steel structure

Ahmed et al. [2] proposed a new form-finding method for cable dome structures to enhance the overall stability of the strut and structure, as well as to minimize the quantity of ring and diagonal cables. Their research results provide a new scheme for the design of cable dome structure. Zhu et al. [3] introduced the extended generalized equilibrium matrix integrated with an equilibrium matrix for cable structures. That research offers innovative ideas and

methods for determining forces in cable structures. Chen et al. [4] developed a nonlinear robustness evaluation method for analyzing and assessing the resilience of cable dome structures, resulting in the achievement of optimized cross-sectional designs. Knawa-Hawryszków [5] presented a numerical analysis approach to determine the initial tension of a two-wire cableway carrying a dynamic load. Their study established an evaluation method for the permissible relative displacement of multi-span load-bearing cables in a double-cableway system with counterweights. Zhao et al. [6] introduced a hybrid optimization algorithm for initial prestress design, highlighting the considerable impact of initial prestress optimization on structural stability.

In the realm of structural design, a majority of research has concentrated on achieving optimal prestress design, shaping, and topology of structures while considering the influence of singular factors [7,8]. An imperative challenge that hampers structural design pertains to the reduction of computational expenses entailed by parametric analysis and adjustment during the design phase. Currently, scant research addresses the attainment of optimum section parameters while maintaining structural integrity. During structural design, the correlation between design parameters (DPs) and the structural safety state remains elusive due to the absence of thorough exploration and fusion of structural DPs with mechanical parameters (MPs). Furthermore, structural design necessitates the simultaneous consideration of numerous variables. Traditional methodologies for structural design encounter difficulties in resolving multi-variable optimization predicaments. Consequently, the sophistication of prestressed steel structure design requires further development.

During the design process, a foundational framework should be established to facilitate the safety assessment of structures during construction, operation, and maintenance [9]. Throughout the entire lifespan of a building, the optimization of structural DPs can then occur in response to load conditions, driven by artificial intelligence. By integrating multiple structural response data, ensuring the safety of the structure and reducing the design cost have become a research hotspot in the context of the transformation and upgrading of the construction industry [10–12].

1.2 The application of an intelligent algorithm in structural analysis

Currently, artificial intelligence has emerged as a focal point of research across diverse domains, including civil engineering, with intelligent algorithms having a central role. These algorithms possess the ability to discern high-level attributes within primary data, thereby facilitating informed decision-making to enhance the dependability and precision of structural analysis [13,14]. Shishegaran et al. [15] employed nonlinear finite element analysis and a surrogate model to investigate the resistance of reinforced concrete panels (RCPs) under blast loading. In their study, multiple regression models were established to accurately predict the maximum deflection of RCPs and to identify the key influencing factors. Ma and Liu [16] developed a prediction model employing a back propagation (BP) neural network for the compressive strength of concrete constrained by carbon-fiber reinforced plastics, thereby imbuing structural performance analysis with heightened intelligence. In the context of tree-like structure design, Zhao et al. [17] introduced a novel form-finding approach grounded in the BP neural network algorithm. Shishegaran et al. [18] improved the prediction model by using a high correlation variable generator in order to efficiently and accurately predict the compressive strength of concrete. In their study, three single models (stepwise regression, gene expression programming, adaptive neuro-fuzzy inference system) and three mixed models were employed for the prediction of the compressive strength of concrete. Chen et al. [19] designed the amalgamation of multi-objective optimization algorithms to configure shield tunneling cross-sections. Vo-Duy et al. [20] embraced the principles of multi-objective optimization in their work on composite beam structure design. Many scholars have applied intelligent algorithms in structural design and mechanical performance analysis [21,22]. Driven by the algorithm, the efficiency and accuracy of the calculation are effectively improved [23], and a reliable tool is provided for solving engineering problems [24].

1.3 Research significance

As deep learning methodologies allow structural design to advance toward greater levels of intelligence. This study introduces an optimization approach for DPs within prestressed steel structures, taking account of the interplay of multiple factors. This approach not only brings together an array of parameters but also effectively facilitates information sharing throughout the entire design, construction, operation and maintenance phases.

In the course of structural design, the BP neural network is employed to fuse DPs with MPs, thereby constructing a high-precision computational model and facilitating data association. Leveraging these data associations, the Random Forest technique can be incorporated to intelligently analyze MPs and discern key DPs that exert significant influence on the variability of diverse MPs. As relationships between vital DPs and MPs have been identified, MPs can be represented via DPs, consequently reducing computational dimensions. The critical DPs of the structure serve as optimization variables, the structure's MPs provide constraint

objectives, and the material cost of the structure is designated as the optimization target. By harmonizing cost and safety considerations, the optimal resolution for structural DPs is realized.

2 Design parameters optimization framework of prestressed steel structure driven by multi-factor fusion

Prestressed cables are introduced into prestressed steel structures. Therefore, it must be prestressed to form a geometric stiffness to withstand external loads [25,26]. In the design of such structures, the establishment of the prestressed configuration, termed as form-finding, takes precedence [27]. In the contemporary context, prevalent techniques for form-finding include the dynamic density method, dynamic relaxation method, and the nonlinear finite element model (FEM) [28]. The design phase of a structure offers a dependable analytical foundation for both the construction and subsequent lifespan operation and maintenance.

Based on the simulation outcomes, the correlations between DPs and MPs can be determined. Taking the simulation results as samples, the deep learning algorithm mines the association rules between data. According to the characteristics of prestressed steel structure, the relationships between DPs and MPs are formed in the design stage of the structure, which is expressed as Eq. (1).

$$f\left(\alpha_1, \alpha_2, \cdots, \alpha_m\right) \overset{R}{\Longleftrightarrow} g\left(\beta_1, \beta_2, \cdots, \beta_n\right), \quad (1)$$

where $f\left(\alpha_1, \alpha_2, \cdots, \alpha_m\right)$ is an aggregation of DPs; and $\alpha_1, \alpha_2, \cdots, \alpha_m$ standed for concrete DPs, including cable sizes, initial tension, respectively. $g\left(\beta_1, \beta_2, \cdots, \beta_n\right)$ denotes an aggregation of MPs, and $\beta_1, \beta_2, \cdots, \beta_n$ refers to specific MPs, such as vertical displacement, stress and tensile force of the cable, respectively. '$\overset{R}{\Longleftrightarrow}$' represented corresponding the relationships between DPs and MPs are established in alignment with technical standards and the structure's data association rules. Guided by these association rules, alterations in DPs lead to modifications in the structure's MPs, thereby facilitating assessment of the structural model's feasibility.

Upon the establishment of associations between DPs and MPs, a numerical proxy model was formulated to represent the structure. The MPs were employed to set the safety conditions of the structure, with safety states categorized based on specific MP values. The extent of impact that different DPs held on the alteration of a given MP was assessed. This facilitated the identification of pivotal DPs influencing the MPs, thus determining a relationship between these key DPs and MPs.

By forging a functional link between MPs and key DPs, a substantial reduction in computational dimensions was realized. Guided by exceeding MPs' permissible limits, accurate corrections were applied to the key DPs. In accordance with the principle of optimal selection, the most suitable structural model was identified by considering the safety performance associated with the structure's MPs, alongside the cost factors tied to the DPs. An overview of the comprehensive parameter optimization methodology is depicted in Fig. 1.

3 Correlation between design parameters and mechanical parameters

Establishing the relationships between DPs and MPs is the first step to realize the optimization of DPs. In this study, according to the bearing capacity of the structure, the MPs corresponding to different DPs are obtained. This process was guided by the application of the BP neural network, culminating in the development of a

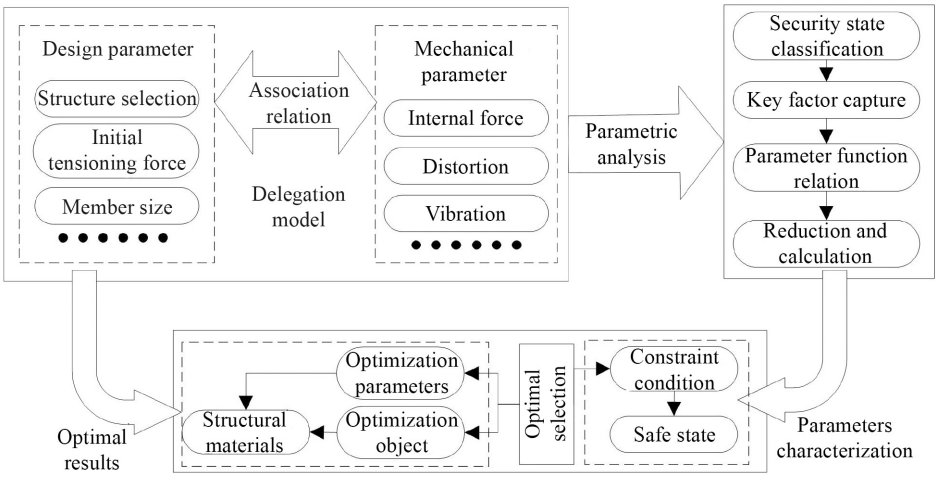

Fig. 1 Multi-factor coupling driven parameter optimization architecture.

parameter correlation model. Embedded within this correlation model, MPs were directly acquired based on given DPs, thereby identifying an inherent connection between these two parameter categories.

An artificial neural network operates as a data mapping model that emulates human brain activities. The task of mapping intricate causal relationships can be accomplished by means of adaptive learning from extensive sample data [29]. There now exists a multitude of artificial neural networks encompassing more than ten varieties, and the most representative one is BP neural network. A BP neural network possesses the capacity to analyze primary data and adaptively process inherent characteristics [30,31] and soit finds widespread application across engineering, finance, the chemical industry, and various other domains, attracting continuous study and optimization efforts [32,33]. Strong linear correlations exist between the parameters of prestressed steel structures. By establishing the relationship between DPs and MPs, the BP neural network can accurately analyze and significantly reduce calculation time.

From a perceptron standpoint, the neural network can be compartmentalized into the input layer, hidden layer, and output layer [34]. The topology of the neural network simulates the interconnections observed between human brain neurons. Activation functions within this network serve as substitutes for human brain neuron connections, enabling analysis and processing, as visually depicted in Fig. 2 [35].

The BP neural network employs a mean square error (*MSE*) driven learning approach for calibration. Through iterative weight adjustments, it ensures the alignment of processing outcomes with the envisioned objective model of the neural network [36].

By examining the foundational principle of the BP neural network, a novel perspective was introduced for optimizing DPs within prestressed steel structures.

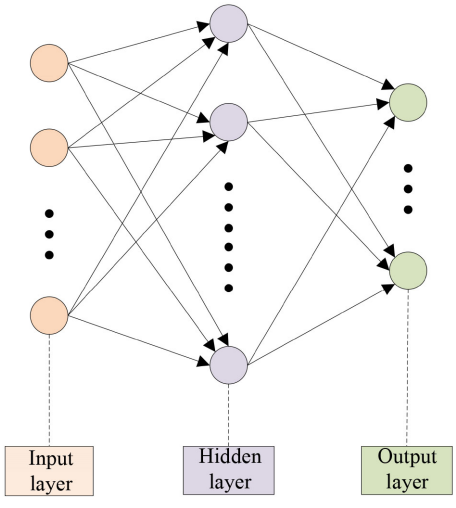

Fig. 2 A diagram of neural network structure.

Throughout the process of structural design in this study, simulations were conducted employing FEM software [37]. Initially, DPs of the structure were designated to modify the design load amalgamation, thereby determining the corresponding MPs. In alignment with China's national technical code governing structures, these MPs were eventually used to assess the viability of form-finding. The selection of DPs and their associated numerical ranges was informed by our engineering expertise.

A wide range of samples was generated during the FEM analysis, encompassing both structural DPs and MPs. The samples constituted a data set that underpinned the construction of a correlation model for structural parameters through the application of the BP neural network. Taking the example of cable truss structures, the confluence of structural DPs and MPs, as explored within this study, is explicitly articulated via Eqs. (2) and (3) [38,39]. In cable truss structures, the mechanical response of cable members serves as a gauge for characterizing the structural safety state [38].

$$DP = \left(N_{\mathrm{sp}},\ D_{\mathrm{urc}},\ D_{\mathrm{lrc}},\ D_{\mathrm{cc}},\ IT_{\mathrm{urc}},\ IT_{\mathrm{lrc}},\ IT_{\mathrm{cc}}\right), \tag{2}$$

$$MP = \left(D_{\mathrm{p}},\ S_{\mathrm{urc}},\ S_{\mathrm{lrc}}\right), \tag{3}$$

where DP stands for an aggregation of DPs of the structure; N_{sp} represents the number of cable trusses; D_{urc}, D_{lrc} and D_{cc} equal the diameters of upper radial cables, lower radial cables and constructional cables, respectively; IT_{urc}, IT_{lrc}, and IT_{cc} are initial tensions of upper radial cables, lower radial cables, and constructional cables, respectively; MP is a set of MPs of the structure; D_{p} denotes the structural vertical displacement; S_{urc} and S_{lrc} refer to stresses of upper and lower radial cables, respectively. The selection of DPs provided the basis for the construction of the simulation model, and the selection of MPs provided the basis for the feasibility of the structural design. Based on the above content, the flow chart of parameter association relationship establishment is shown in Fig. 3.

Leveraging the architectural attributes of the BP neural network and the principles of structure design, diverse types of DPs were categorized as constituents of the network's input layer. Concurrently, various MPs were classified as components of the output layer. These corresponding MPs were generated through the specification of DPs and design load conditions within the FEM framework. The MPs derived from FEM analysis served as a pivotal reference for assessing the accuracy of the neural network.

Guided by the DPs, anticipated MPs were garnered by inputting them into the neural network model. Through a comparative analysis of the MPs generated by the two

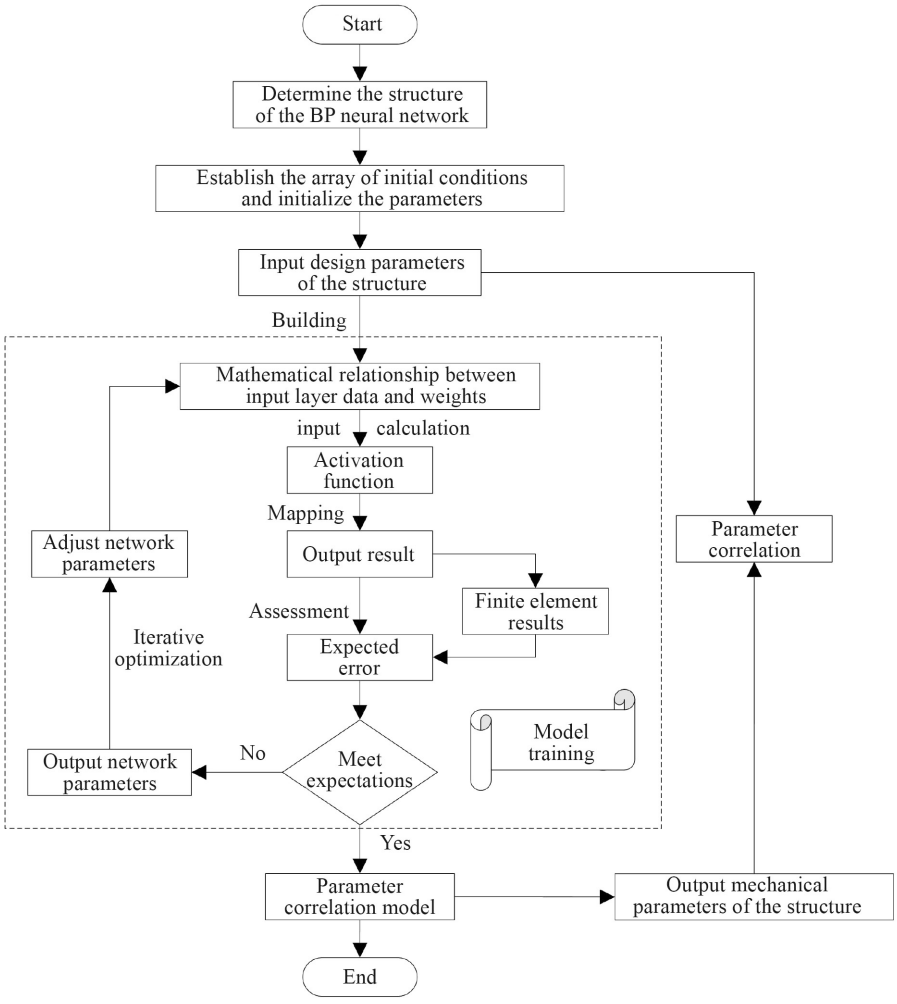

Fig. 3 The process of establishing parameter association relationship.

methodologies, the weight of the prediction model underwent continual refinement. This culminated in the formulation of a dependable parameter correlation model. Within this model, the interconnected relationship between the input DPs and the resultant output MPs was explicitly defined, thus giving rise to the configuration of parameter correlations. This intricate interplay of parameter correlations, in turn, underpinned the scrutiny of structural mechanical attributes.

4 Analysis of mechanical properties of prestressed structures

Guided by the interplay of parametric connections, the reciprocal relationships between DPs and MPs were elucidated. The classification of MPs facilitated the evaluation of the structural design's feasibility. Empowered by classification algorithms, pivotal factors influencing fluctuations in specific MPs were identified, thereby providing a foundational framework for ensuring structural safety across the construction, operation, and maintenance phases.

4.1 Mechanical parametric analysis model

By configuring distinct sample training sets, the Random Forest algorithm is able to undertake an analysis of data classification [40,41]. This entails the acquisition of a sequence of classification models through K rounds of training. A multi-classification model system is thereby established, and the ultimate classification outcomes are determined via straightforward majority voting decisions. The resultant classification decision can be succinctly articulated as demonstrated in Eq. (4).

$$H(x) = \underset{Y}{\operatorname{argmax}} \sum_{i=1}^{K} I(h_i(x) = Y), \tag{4}$$

where $H(x)$ refers to the combinatorial classification model; h_i denotes individual decision tree models, Y respresents output variables, and $I(\cdot)$ shows indicator functions. In the process of constructing the Random Forest classification algorithm, it was necessary to set the number of decision trees and the maximum number of features to ensure that the model was optimal.

Based on the derived robust correlation model, showing

good predictive capabilities, the MPs were amalgamated with the Random Forest algorithm. Concurrently, safety levels were stratified in alignment with specific MP values. These safety levels, along with their associated DPs, were integrated into the Random Forest decision model. This process culminated in the establishment of a mechanical analytical model. Applying this model, the safety level of the structure corresponding to the DPs was intelligently evaluated, thereby identifying the pivotal DPs that exert influence over the structure's safety.

4.2 Analysis of structural mechanical properties

The integration of MPs with the Random Forest technique laid a solid groundwork for analyzing the mechanical behavior of the structure. During the design of the structure, MPs were generated by means of DPs and analyses of loading conditions. These MPs played a pivotal role in characterizing the structural safety and dependability.

To illustrate, the cable truss structure was adopted to delineate three distinct categories of MPs, as denoted in Eq. (3). Specifically, these parameters were categorized into four tiers of levels (A, B, C, D). Subsequently, the performance levels aligned with diverse DPs were employed as both the input and output of the mechanical analytical model. Through the utilization of the random forest method, an intelligent scrutiny of the structure's mechanical performance took place, enabling the estimation of its safety. During these analyses, the varying impacts of different DPs were meticulously determined in relation to the fluctuations observed across an array of MPs.

In assessments of the mechanical performance of the prestressed steel structure, data samples were collected by means of mechanical analyses according to associations of DPs and MPs, and MP's classifications. Among these samples, DPs and safety levels were respectively used as input and output elements. The acquisition of such samples can be expressed in Eq. (5).

$$DP \overset{MP}{\Rightarrow} \begin{cases} \overset{D_{\mathrm{p}}}{\rightarrow} (A,\ B,\ C,\ D), \\ \overset{S_{\mathrm{urc}}}{\rightarrow} (A,\ B,\ C,\ D), \\ \overset{S_{\mathrm{lrc}}}{\rightarrow} (A,\ B,\ C,\ D). \end{cases} \tag{5}$$

Using the collected samples, the analytical model's training and testing sets were demarcated. By way of the Random Forest approach, hyper-parameters were finetuned to fabricate a high-precision mechanical performance analytical model. The grade of various MPs can be judged by designing parameters, and the key factors affecting the change of various MPs can be obtained. Furthermore, critical factors governing variations in MPs were discerned. By referencing the classification of MPs and the pivotal influencing factors, the safety assessment of the structure was effectively ensured. The structural mechanical properties' analytical process is visualized in Fig. 4.

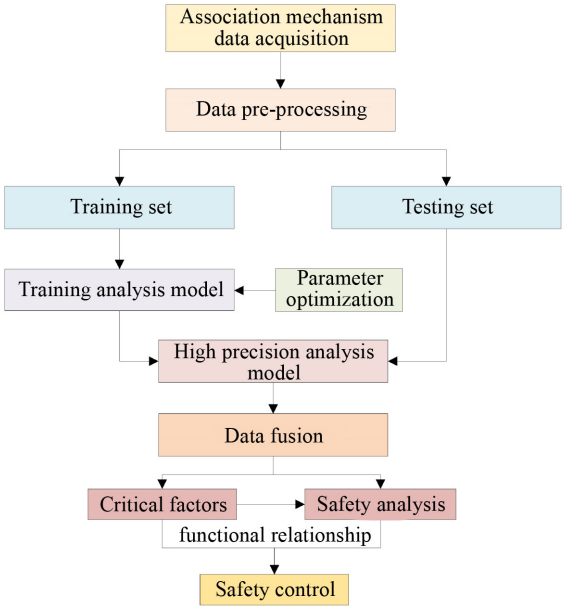

Fig. 4 The structure's mechanical performance analysis process.

5 Optimal selection of structural design parameters

Driven by the concept of objective optimization [42], DPs and MPs were integrated to optimize the structure. In this study, the feasibility of the design was considered from the two aspects of cost factor and safety factor. The cost factor of structural design was characterized by the DPs, and the safety factor was characterized by the MPs. The aim was that optimal design of the structure would minimize the cost on the basis of meeting the safety performance requirements. The optimal design idea of the structure is expressed as Eq. (6).

$$O.F. = \min\left(f_1(x),\ f_2(x),\ \cdots,\ f_{\mathrm{p}}(x)\right), \tag{6}$$

$$\text{s.t. } D_{\mathrm{p}} \leqslant a,\ b \leqslant S_{\mathrm{urc}} \leqslant c,\ d \leqslant S_{\mathrm{lrc}} \leqslant e,$$

In Eq. (6), '$O.F.$' represents the objective function, that is, the minimum cost. $f_i(x)$ represents costs corresponding to different varieties of DPs. Optimized parameters during optimization are DPs of the structure. The constraint condition (s.t.) represents the safety performance of the structure. In this study, three categories of important MPs were selected to evaluate safety performance, that is vertical displacement (D_{p}), upper radial cable stress (S_{urc}) and lower radial cable

stress (S_{lrc}). They were all functions of DPs. Concerning constraints, the maximum vertical displacement a was determined according to technical specifications and engineering experience [43,44]. The maximum and minimum values (b, c, d, and e) of the upper radial cable and the lower radial cable forces were set to ensure that the structure did not relax and the stress was not too large during construction, operation, or maintenance. Both cost factors and safety factors were related to DPs, so the essential purpose of optimization was to select the DPs that ensure structural safety and minimize the cost.

Driven by genetic algorithm (GA) [45], the objective function and constraint conditions were formed. Through a combination of DPs and MPs, the influence of cost and safety factors on structure design was duly considered. Thus, the optimal selection mode of structure design was formed and the DPs of the structure were determined. The optimal selection of structural DPs based on GA is shown in Fig. 5.

GA was employed in the pursuit of optimal parameter selection. By combining the outcomes of the Random Forest approach and MPs, the significance of various factors that affect the safety performance of the structure was assessed. This evaluation enabled the identification of representative DPs, which were then formulated to express the relationship between parameters and structural safety. This expression was subsequently adopted as the constraint for optimization selection.

Simultaneously, a functional relationship between DPs and material costs was established and deemed the optimization objective. Guided by the GA, the eventual outcome was the attainment of an optimal solution. The spectrum of DPs corresponding to this optimal solution constitutes the culmination of the optimization process.

6 Case study

Drawing upon the distinctive attributes of prestressed steel structures, an optimization methodology for DPs was introduced. This methodology engendered the establishment of a connection between DPs and MPs. By leveraging intelligent analyses of mechanical characteristics, an understanding of the interplay between these two categories of parameters was established. This culminated in the derivation of an optimal structural design solution in terms of considerations of both cost and safety.

To demonstrate the efficacy of the proposed approach, a real-world application in the design process of a spoke cable truss structure was examined as an illustrative example.

6.1 Form of the structure

The studied structure was a gymnasium with a span of 80 m, including columns, ring beams, radial cables and vertical cables. The columns and the ring beam were steel components. The ring beams were further divided into upper inner ring beam, lower inner ring beam and outer ring beam. The upper and lower inner ring beams were connected with flying columns. Radial cables consisted of upper and lower radial cables that were connected with inner and outer vertical cables. The allowable stress of cables was set at 1670 MPa. According to the architectural design requirements, the diameter of the inner ring beam was 10 m, the height of the flying column was 10 m, and the height of the outer column was 20 m. The structure form of the gymnasium is shown in Fig. 6.

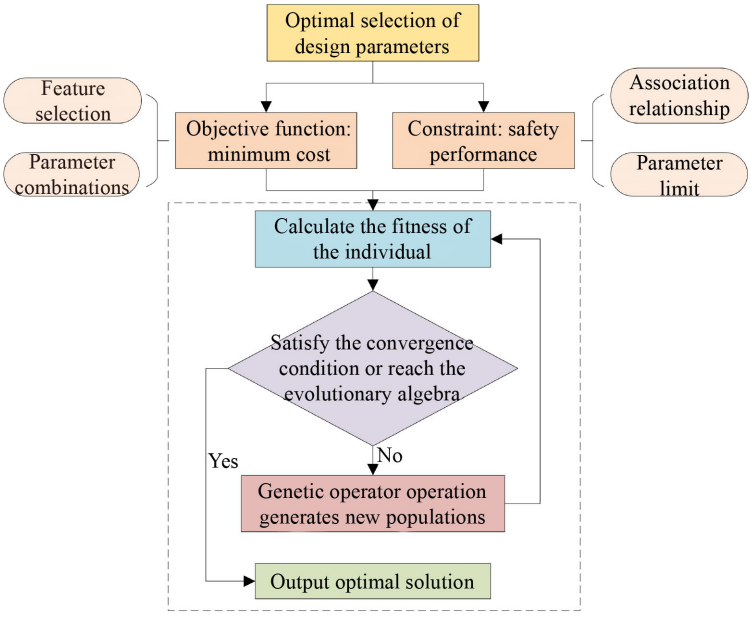

Fig. 5 GA-based optimum selection of structure DPs.

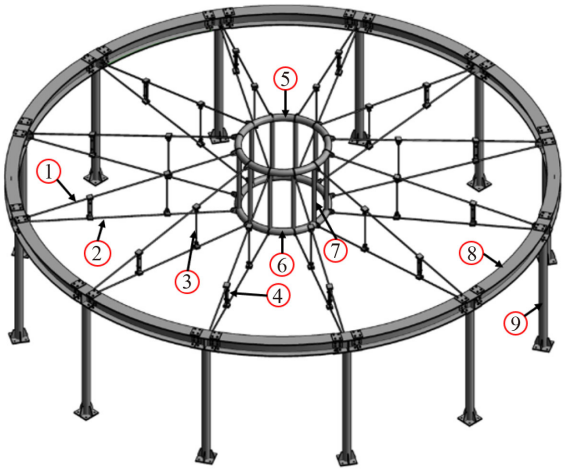

Fig. 6 Structure style of the gymnasium (① upper radial cable, ② lower radial cable, ③ inner vertical cable, ④ outer vertical cable, ⑤ upper inner ring beam, ⑥ lower inner ring beam, ⑦ flying column, ⑧ outer ring beam, ⑨ outer column).

In the process of structural design optimization, the number of the cables trusses, the diameter of the radial cables, the diameters of the vertical cables, the initial tensions of the radial cables, and the initial tensions of the vertical cables were taken as the DPs of the structure. A cable truss included an upper radial cable, a lower radial cable and a connected vertical cable. According to the DPs, the MPs of the structure can be generated by setting the design load combination in the FEM. The main MPs analyzed in this study were the vertical displacement, the stress of the upper radial cable and the stress of the lower radial cable.

In the design process of the structure, the mechanical analysis model was established by the finite element software ANSYS. In ANSYS, the cables were established by the Link167 elements assuming linear elastic material behavior, and the ring beam and columns were established by the Beam188 elements assuming elastic-perfectly plastic material behavior [46]. The MPs of the structure were obtained in the mechanical analysis model to provide samples for the training of the numerical simulation. The relationship between DPs and MPs was established in BP neural network. Seven main DPs were selected based on sensitivity analysis. Taking the above seven DPs as input parameters, the BP neural network characteristics for accurately predicting the three DPs were established respectively. The neural network established the relationship under specific loads. For example, under the limit state of normal use, the relationships between DPs and MPs were obtained. The MPs were discretized, and different intervals were divided to characterize the safety level of the structure, and the key DPs were obtained. By establishing the functional relationship between MPs and key DPs, the dimension of calculation was effectively reduced. In accordance with the principle of optimal selection, the most suitable structural MPs was selected by considering the safety performance associated with the structure's MPs, alongside the cost factors tied to the DPs.

6.2 Comparative analysis of geometric form

Throughout the process of structural design, the interrelation between DPs and MPs was affirmed through FEM analyses. Guided by the BP neural network, a parameter correlation relationship was conceived, thereby cementing the linkage between DPs and MPs. Subsequently, an intelligent analysis of the structure's mechanical behavior was conducted by considering its MPs.

6.2.1 Parameter association rule acquisition

Derived from the dissection of the fundamental principle of the BP neural network, as explained in Subsection 3.1, the correlation relationship for the prestressed steel structure was established, with DPs and MPs functioning as the input and output layers, respectively. To serve as training samples for the associational relationship, data garnered from the finite element analysis under the self-weight condition of the structure was assimilated. The determination of the neuron count within the hidden layer could be computed according to Eq. (7) [47].

$$l = \sqrt{n+m}+a, \tag{7}$$

where l refers to the number of hidden layer neurons; n denotes the number of input layer neurons (i.e., the number of DPs types); m respresents the number of output layer neurons (i.e., the number of MPs types); a is a constant ranging from 1 to 10. The BP neural network had an iteration number of 6000, and its learning rate was 0.035. In addition, *MSE* was selected as a function to evaluate model performance. In the event of $MSE \leqslant 6.5 \times 10^{-4}$, the iteration ended. In the process of designing this structure, three correlation relationships of vertical displacement, and upper and lower radial cable stresses were constructed in correspondence to DPs. According to the architectural design requirements and engineering experience, the values of the seven types of DPs are shown in Table 1. Moreover, the initial tension of the cable is strongly related to the section size [48].

Depending on the value of DPs, many samples were formed under the condition of self-weight. In the process of training the correlation relationship, the influence of the number of different hidden layer neurons on the number of iterations was discussed. If $MSE \leqslant 6.5 \times 10^{-4}$, the model stopped iteration. In this study, the effects of seven types of DPs on vertical displacement, upper radial cable stress and lower radial cable stress were studied. Therefore, referring to Eq. (7), $n = 7$ and $m = 1$ in each neural network. As expressed in Eq. (7), ten integers

ranging from 4 to 13 were taken for l in individual neural networks. The influence of the number of different hidden layer neurons on the number of iterations is shown in Fig. 7.

According to Fig. 7, for the prediction of vertical displacement, upper radial cable stress and lower radial cable stress, 6 and 8 hidden layer nodes had the least number of iterations. Figures 8–10 show the comparison between the predicted MPs output of the correlation model under the condition of dead weight and the actual MPs of the FEM analysis.

Similarly, an analogous relationship was constructed within a load combination scenario to undertake a feasibility analysis of the structure. Based on relevant load specifications, this investigation focused on assessing the impact of loads on the structure's vertical orientation [49,50]. The effects of dead load, live load, temperature action and wind action were fully considered in the process of structural design, and 15 kinds of load combination analysis were carried out. Notably, the load combination cases chosen for ultimate states are enumerated in Table 2.

The MPs acquired through assessments under self-weight conditions demonstrated that the associated vertical displacement was notably significant when the number of cable trusses was 10 within the structure. Consequently, MPs aligned with the DPs of the 12 cable trusses were subjected to analysis under combined loading circumstances. Adhering to structural design criteria, an evaluation of cable stress was conducted to determine its agreement with the ultimate limit state.

Similarly, the rationality of vertical displacement was evaluated in light of the serviceability limit state. Notably, Loading Conditions 1 and 3 proved unfavorable in both the aforementioned states. As a final step, the

Table 1 A table of values assigned to DPs

Parameter type	Value
Cable number	10, 12
Upper radial cable diameter (mm)	60, 70, 80, 90, 100
Lower radial cable diameter (mm)	60, 70, 80, 90, 100
Vertical cable diameter (mm)	30, 40, 50
Initial tension of upper radial cable (kN)	800, 850, 900, 950, 1000
Initial tension of lower radial cable (kN)	800, 850, 900, 950, 1000
Initial tension of vertical cable (kN)	200, 250, 300

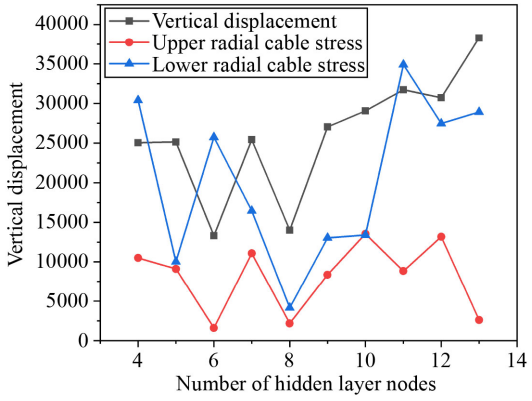

Fig. 7 Impacts of different numbers of hidden layer neurons on the iteration number.

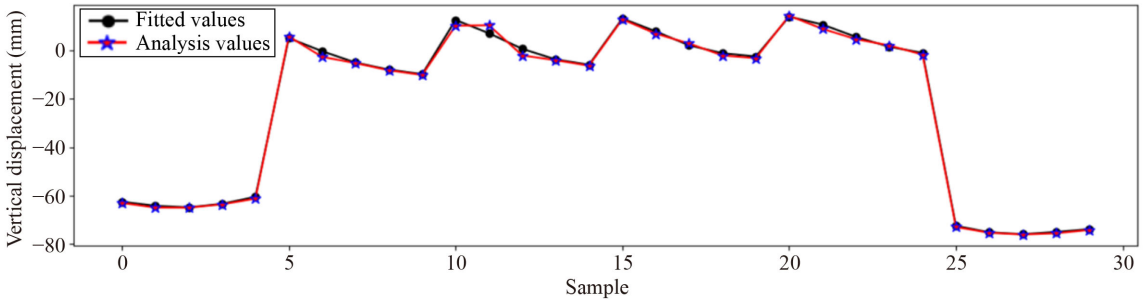

Fig. 8 Comparison between vertical displacement of model output and vertical displacement of FEM analysis (partial sample).

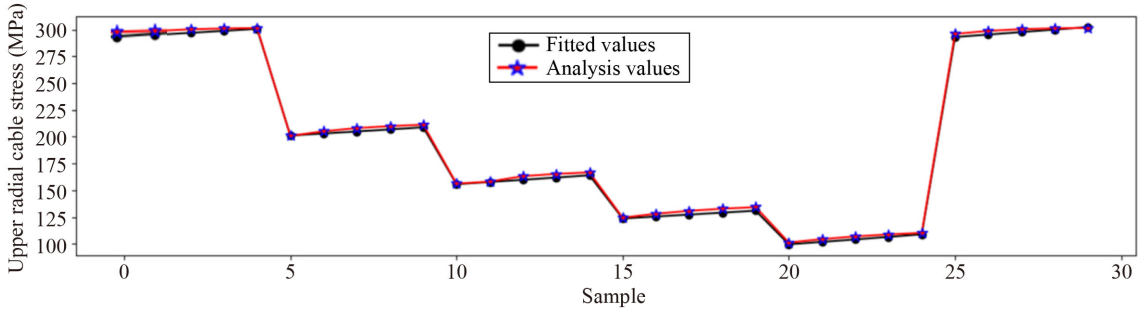

Fig. 9 Comparison between upper radial cable stress of model output and that of FEM analysis (partial sample).

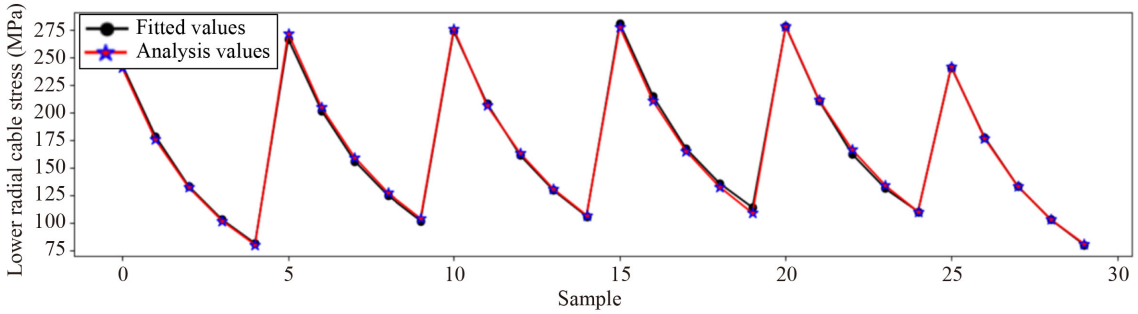

Fig. 10 Comparison of lower radial cable stress from model output and lower radial cable stress from FEM analysis (partial sample).

Table 2 Load combination cases

Limiting condition	Loading condition number	Loading condition
Ultimate limit state	Loading Condition 1	1.3 × (constant load + prestress) + 1.5 × live load
	Loading Condition 2	1.3 × (constant load + prestress) + 1.5 × wind load
Serviceability limit state	Loading Condition 3	1.0 × (constant load + prestress) + 1.0 × live load
	Loading Condition 4	1.0 × (constant load + prestress) + 1.0 × wind load

parameter correlation relationship under these two working conditions was formulated. To ascertain the validity of the relationship, the MPs it generated were juxtaposed with the outcomes of FEM analysis, as illustrated in Figs. 11–13. The comparison results showed that the BP neural network can accurately establish the correlation relationships between DPs and MPs. Consequently, this facilitated intelligent structural design and feasibility analysis by inputting DPs, thus markedly enhancing the efficiency of structural design. Furthermore, the contrast between the two loading conditions underscored the heightened adversity of Loading Condition 1, emphasizing the imperative of concentrating on structural performance within this specific loading scenario.

6.2.2 Analysis of structural mechanical properties

Driven by associations of DPs and MPs, the random forest was integrated to analyze the structural mechanical

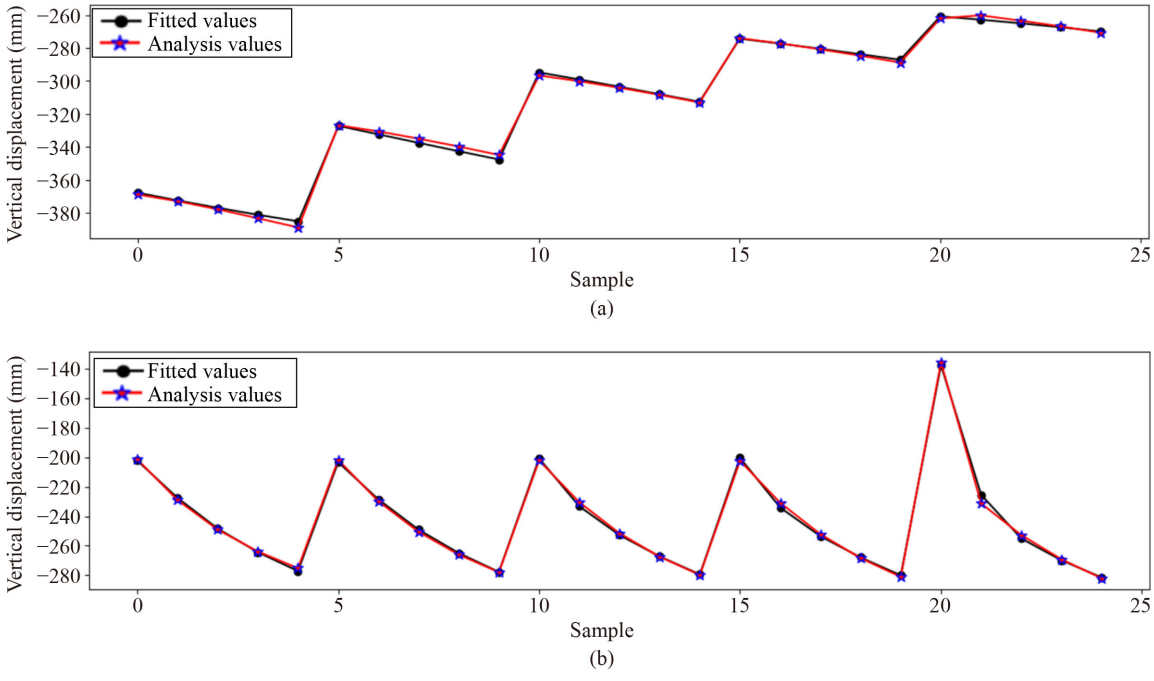

Fig. 11 Comparison of vertical displacement obtained by the model with that of FEM analysis (partial samples): (a) comparison under the action of Loading Condition 1; (b) comparison under the action of Loading Condition 3.

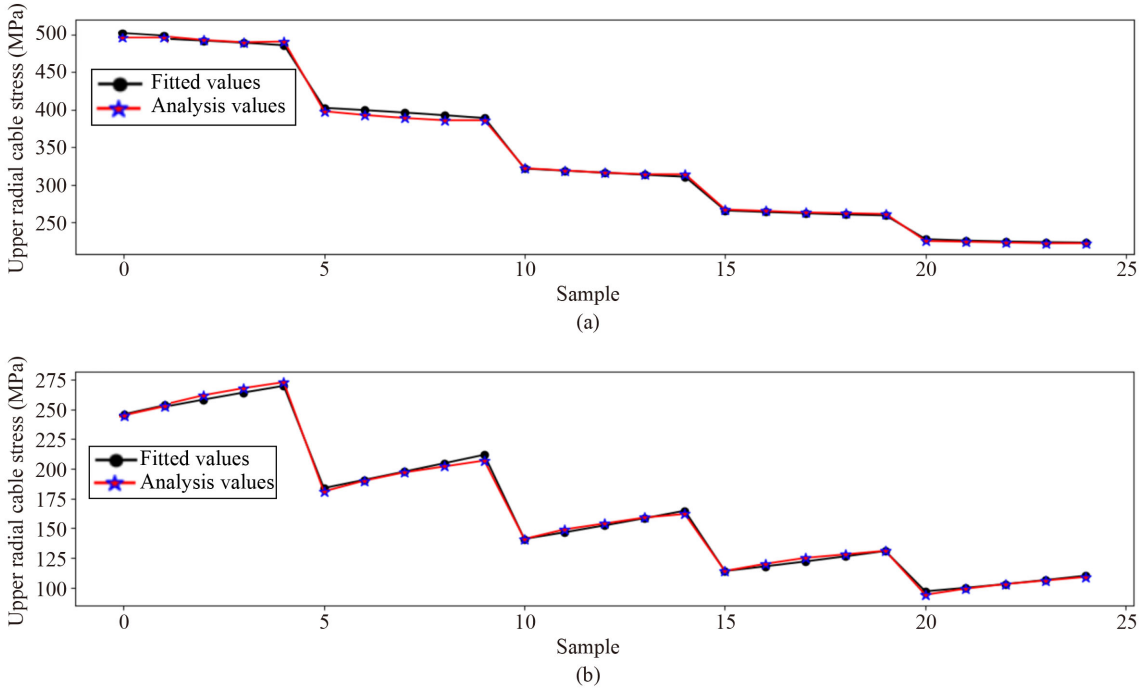

Fig. 12 Comparison of upper radial cable stress obtained by the model with that of FEM analysis (partial samples): (a) comparison under the action of Loading Condition 1; (b) comparison under the action of Loading Condition 3.

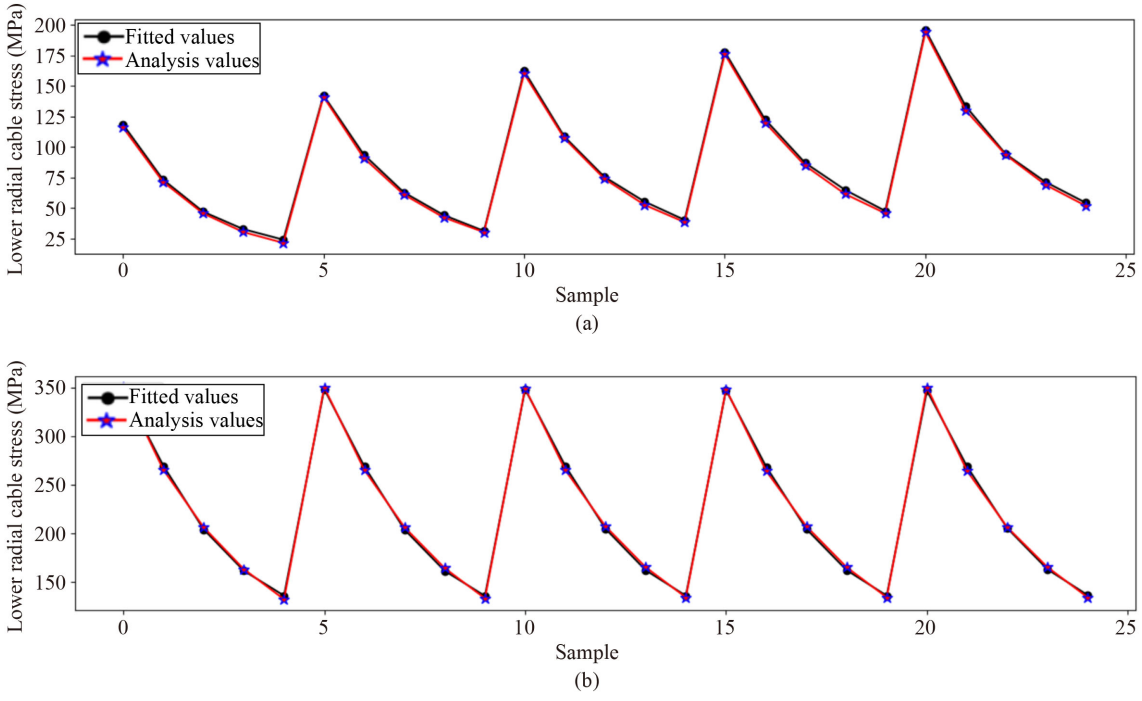

Fig. 13 Comparison of lower radial cable stress obtained by the model with that of FEM analysis (partial samples): (a) comparison under the action of Loading Condition 1; (b) comparison under the action of Loading Condition 3.

performance. According to the flow diagram of analysis described in Subsection 4.2, all kinds of MPs were first classified (Table 3). Based on the conclusion of Subsubsection 6.2.1, the mechanical properties of the structure under the action of Loading Condition 1 were analyzed.

During the course of analyzing mechanical properties, distinct analysis models for vertical displacement, upper radial cable stress, and lower radial cable stress were individually established. Guided by the principles of the random forest methodology, DPs and the levels of MPs were used as input layer and output layer of the model.

Table 3 Classification of MPs

Parameter type	Structural safety rating	Parameter range
Vertical displacement	A	[−212.5 mm, −150 mm)
	B	[−275 mm, −212.5 mm)
	C	[−337.5 mm, −275 mm)
	D	[−400 mm, −337.5 mm]
Upper radial cable stress	A	[200 MPa,275 MPa)
	B	[275 MPa,350 MPa)
	C	[350 MPa,425 MPa)
	D	[425 MPa,500 MPa]
Lower radial cable stress	A	[0 MPa,50 MPa)
	B	[50 MPa,100 MPa)
	C	[100 MPa,150 MPa)
	D	[150 MPa,200 MPa]

Via comprehensive model analysis, the pivotal factors (DPs) responsible for driving alterations in diverse MPs were distinctly identified, as illustrated in Fig. 14.

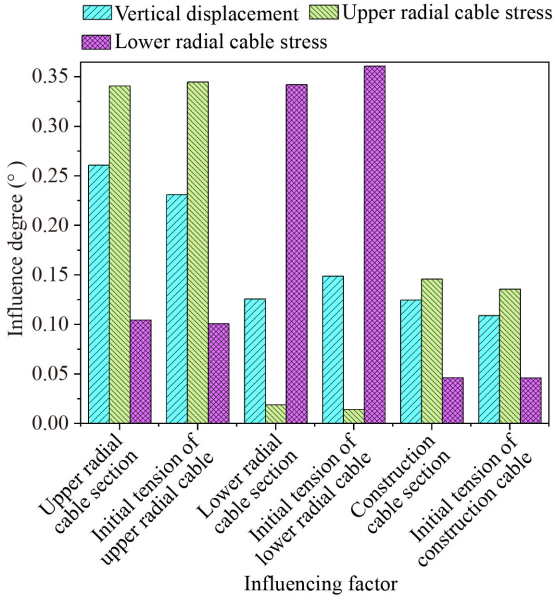

Fig. 14 Influence degrees of DPs on MPs.

In Fig. 14, the prominent factors influencing variations in the MPs of the structure are visually evident. Notably, the cross-sectional dimensions of the radial cables exerted the most substantial influence on vertical displacement. Furthermore, the initial tension and cross-sectional size of the upper radial cable exhibited the most pronounced impact on the stress distribution in the upper radial cable. Similarly, the initial tension and cross-sectional size of the lower radial cable held the greatest sway over the stress distribution in the lower radial cable. As a result, in cases where certain MPs of the structure surpass acceptable limits, corrective measures can be implemented by addressing these pivotal influencing factors. In addition, the cable's cross-sectional area showed a correlation with its initial tension, and in Fig. 14, the comparable influence of these two factors on MPs implies the dependability of the analysis model developed within this study. Through the comprehensive analysis of the structure's mechanical properties, a foundation was established for the safety assessment of the structure throughout its construction, operation, and maintenance phases. This research methodology, to a considerable extent, achieved the integration of information sharing across the entire lifecycle of the building.

6.3 Optimal selection of structural design parameters

The ultimate step in achieving an intelligent structural design was the optimal parameter selection. In the design progression of the experimental structure, the most favorable configuration of DPs was derived through a multi-objective optimization approach. Guided by the theoretical methodologies outlined in Section 5, the conclusive decisions could be reached by integrating both cost and safety considerations. By adhering to the relationship between DPs and MPs, a corresponding data set could be obtained. This data set encompassed the MPs that correlated with specific DPs. During the optimization selection phase, the data set was employed as a benchmark, particularly under the influence of Loading Condition 1. In accordance with the DPs−MPs connection established via the BP neural network, it was determined that the number of cable truss was 12 resulted in a more tenable force distribution. Leveraging the insights from the Random Forest analysis, the initial tension of diverse cables corresponded proportionally with their cross-sectional areas. As a consequence, the impact on the structure's mechanical attributes remained consistent across the spectrum. In this study, the selected optimization parameters were the diameter of the upper radial cable (D_{urc}), the diameter of the lower radial cable (D_{lrc}) and the diameter of the construction cable (D_{cc}). The optimization objective in the mathematical model (Eq. (6)) was cost ($\bar{\omega}$). According to the project budget, the mathematical expression of cost and DPs is Eq. (8).

$$\bar{\omega} = k\rho \times \frac{\pi}{4}\left(D_{\mathrm{urc}}^2 l_1 + D_{\mathrm{lrc}}^2 l_2 + D_{\mathrm{cc}}^2 l_3\right), \tag{8}$$

where k stands for the cost incurred by the structure in unit mass (10 RMB/kg); ρ denotes density of cable materials, that is 7.85×10^{-6} kg/mm^3. In addition, l_1, l_2, and l_3 refer to the length of three types of cables, 36278, 36278, and 4644 mm, respectively. The cost of the structure was proportional to the diameter of various cables. If the size of the cable was too small, it did not meet the required safety performance. According to the technical specification [43,44], the vertical displacement of the structure should not exceed 1/250 of the span, that

is, 320 mm. The stress of the cable should not exceed 0.4 times of the allowable stress, that is, 668 MPa. To ensure the normal structure construction, operation and maintenance, the cable relaxation requirements should be met, and the lower limit of the cable stress was selected to be 100 MPa. The optimal selection range of DPs, as driven by GA, is shown in Table 4.

Table 4 Optimal selection range of DPs

DP	Value range
Upper radial cable diameter	[60 mm,100 mm]
Lower radial cable diameter	[60 mm,100 mm]
Constructional cable diameter	[30 mm,50 mm]

To satisfy the required structural safety performance, particular emphasis was placed on analyzing Loading Condition 1. This enabled the acquisition of the corresponding MPs from the DPs. Facilitated by the BP neural network, a robust correlation between these two sets of parameters was established. Subsequently, through the application of Random Forest analysis, the pivotal DPs influencing the diverse MPs were extracted from data as shown in Fig. 14.

To visually depict the connection between MPs and DPs, a graphical representation illustrating the relationship between these two categories of parameters was formulated, as depicted in Fig. 15. Concerning the impact on displacement, the key factors selected primarily included the diameters of the upper radial cable and the lower radial cable. Similarly, for the effect on upper radial cable stress, the diameters of the upper radial cable along with the vertical cables played a predominant role. As for the influence on the lower radial cable, the diameters of the upper radial cable and of the lower radial cable emerged as the principal factors.

Guided by the DPs and their corresponding MPs, a mathematical linkage between these two types of parameters was established and are documented in Table 5.

In Table 5, the goodness of fit of functions was close to 1. Therefore, the linear fitting method applied in this study met the accuracy requirements. The function expressions of MPs and DPs are specifically expressed as Eqs. (9)–(11). According to the technical regulations, the limit values of the MPs in the structure are specified in the equations.

$$D_{\mathrm{p}} = -381.09728 + 2.75068D_{\mathrm{urc}} - 0.1041D_{\mathrm{lrc}} - 1.10263D_{\mathrm{cc}} \leqslant 320, \tag{9}$$

$$100 \leqslant S_{\mathrm{urc}} = 858.4 - 8.036D_{\mathrm{urc}} - 0.424D_{\mathrm{lrc}} + 3.52D_{\mathrm{cc}} \leqslant 668, \tag{10}$$

$$100 \leqslant S_{\mathrm{lrc}} = 188.00533 + 1.38867D_{\mathrm{urc}} - 2.7194D_{\mathrm{lrc}} - 0.3613D_{\mathrm{cc}} \leqslant 668. \tag{11}$$

As detailed in Section 5, optimization of structural DPs was conducted employing a GA approach. Equation (8) was utilized as the objective function for optimization, whereas Eqs. (9)–(11) were employed as constraint conditions. The permissible value range for the three DPs is outlined in Table 4. Driven by the GA, the process of cost optimization is illustrated in Fig. 16. Through iterative procedures, DPs that ensure both structural integrity and cost efficiency were ultimately identified. Under the designated load conditions stipulated by the design specifications, the MPs derived from this method exhibited a strong alignment with results obtained through FEM calculations, thereby validating the efficacy of the design methodology.

The optimal configuration of DPs generated via this research methodology, alongside the corresponding MPs under Loading Condition 1, are presented in Tables 6 and 7. In contrast, traditional design approaches primarily focus on structural safety considerations. In such approaches, the radial cable diameter is typically around 90 mm, while the vertical cable diameter tends to be approximately 30mm. In contrast, the advanced intelligent design method fully takes into account cost factors, achieving a reduction in material utilization exceeding 20% while still ensuring structural soundness.

For large-scale prestressed steel structure designs, conventional methodologies often require around 200 h for model calculations and optimization. Remarkably, the intelligent design approach proposed in this study slashes this timeframe to a mere 18 h, thereby compressing the design cycle time by over 90%. Furthermore, this innovative design methodology has the potential to provide valuable guidance for the intelligent optimization of analogous structures. To summarize, the proposed intelligent design approach for prestressed steel structures offers the distinct benefits of elevated efficiency, abbreviated timeline, and reduced human resource input.

6.4 Experimental verification

To further corroborate the viability of the proposed theoretical approach, a scale model was constructed based on the architectural configuration detailed in Subsection 6.1. This scale model was calibrated with a geometric ratio of 1:10 relative to the actual engineering dimensions, while the cable's cross-sectional area was scaled down at a 1:100 ratio relative to the genuine engineering structure. The material similarity coefficient remained at 1:1, with the same material composition utilized as in the actual engineering construction. Stress distribution was also rendered proportionately, maintaining a ratio of 1:1 between the test model and the full-scale project. Specifically, Loading Condition 1 was emulated within the test model, enabling the collection of pertinent MPs, such as cable tension and structural

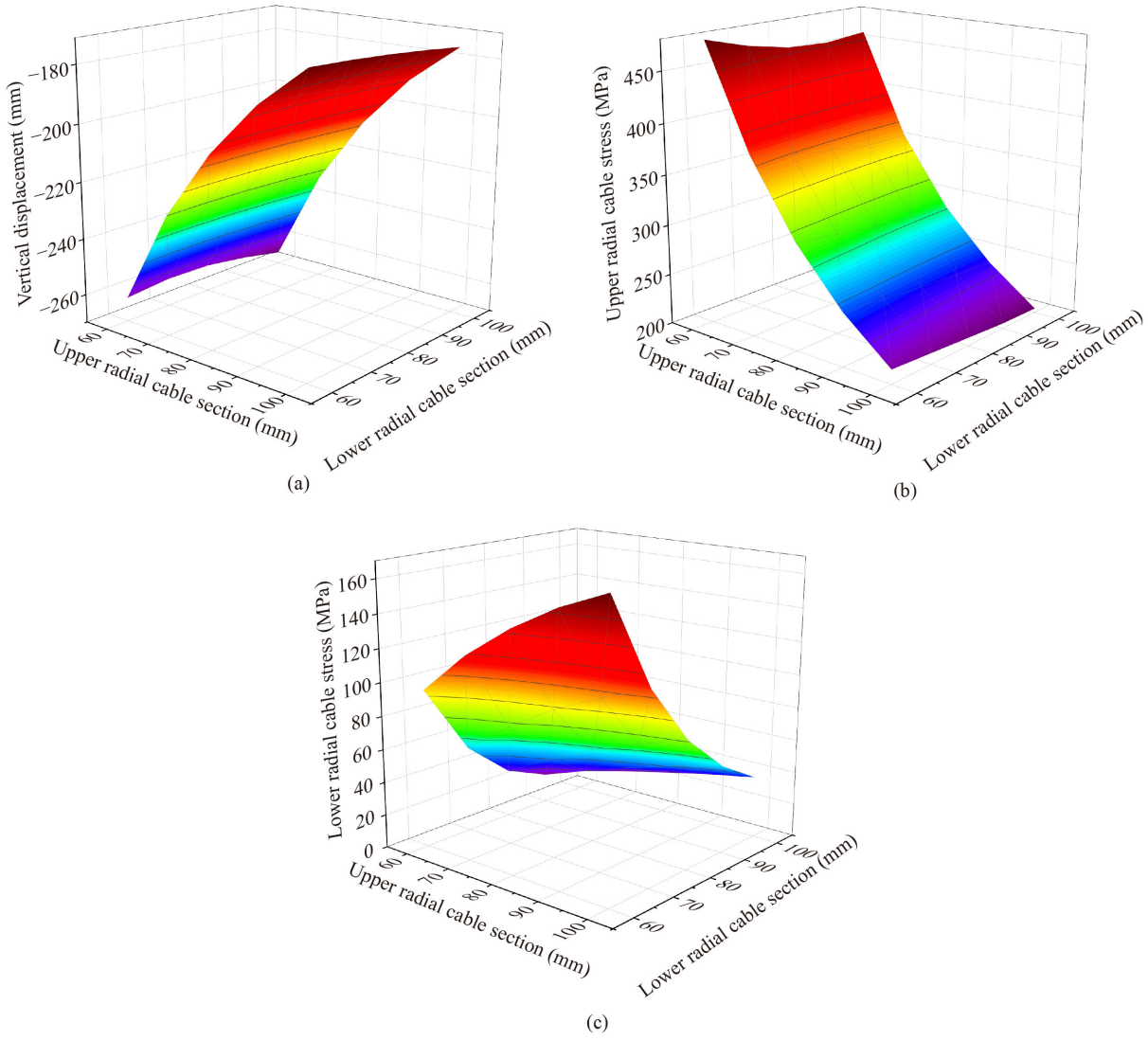

Fig. 15 Relationship between MPs and key DPs: (a) relationship between DPs and vertical displacement; (b) relationship between DPs and upper radial cable stress; (c) relationship between DPs and lower radial cable stress.

Table 5 The properties and goodness of fit for MPs and DPs

MP	Intercept	Upper radial cable diameter	Lower radial cable diameter	Constructional cable diameter	Goodness of fit
Vertical displacement	−381.09728	2.75068	−0.1041	−1.10263	0.97502
Upper radial cable stress	858.4	−8.036	−0.424	3.52	0.96778
Lower radial cable stress	188.00533	1.38867	−2.7194	−0.3613	0.97216

displacement. The configuration of the test model and the arrangement of the imposed loads are visualized in Fig. 17.

Under Loading Condition 1, the comparison between the fitting value of structural MPs and the measured value is shown in Fig. 18, demonstrating that the parameter correlation formed in this study can accurately and effectively analyze the mechanical properties of the structure, with accuracy higher than 95%. Therefore, this research method can realize real-time analysis and accurate prediction of structural mechanical properties, and reduce the dependence on test data.

7 Discussion

This study formed a data association-parameter analysis-optimization selection system for prestressed steel structures. According to the importance analysis of the parameters, the number of structural components, the diameter of the upper radial cable, the diameter of the lower radial cable, the diameter of the vertiacl cable, the initial tension of the upper radial cable, the initial tension of the lower radial cable, and the initial tension of the vertical cable are selected as the DPs. Prediction models of three MPs were established for various working

conditions, and the relationship between DPs and MPs was established. The resulting correlation could quickly and accurately determine the mechanical properties of the structure. Many data mining algorithms are not suitable for continuous data, so data discretization was an indispensable preprocessing step before data mining [51]. According to the requirements of architectural design, the specific value range of DPs was selected. However, the analysis results showed that the MPs output by the neural network model were highly consistent with the measured values of the structural experiment. Therefore, the established neural network had strong analysis accuracy. For the design of large prestressed steel structure, engineers usually needed 200 h to calculate and optimize the model. The intelligent design method proposed in this study only took 18 h; the design cycle time was shortened by more than 90%. According to the specific values of

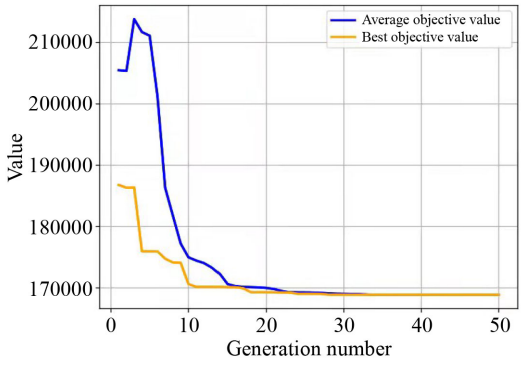

Fig. 16 Parameter optimization process driven by GA.

Table 6 DPs corresponding to the optimum solution

Cable type	Diameter of section (mm)	Corresponding initial tension (kN)
Upper radial cable	70	850
Lower radial cable	60	800
Constructional cable	30	200

Table 7 MPs corresponding to the optimum solution

MP	Vertical displacement (mm)	Upper radial cable stress (MPa)	Lower radial cable stress (MPa)
FEM analysis result	−228.2	378.1	121.9
Correlation fitting results	−227.6	376.0	125.7

Fig. 17 Test model and load arrangement.

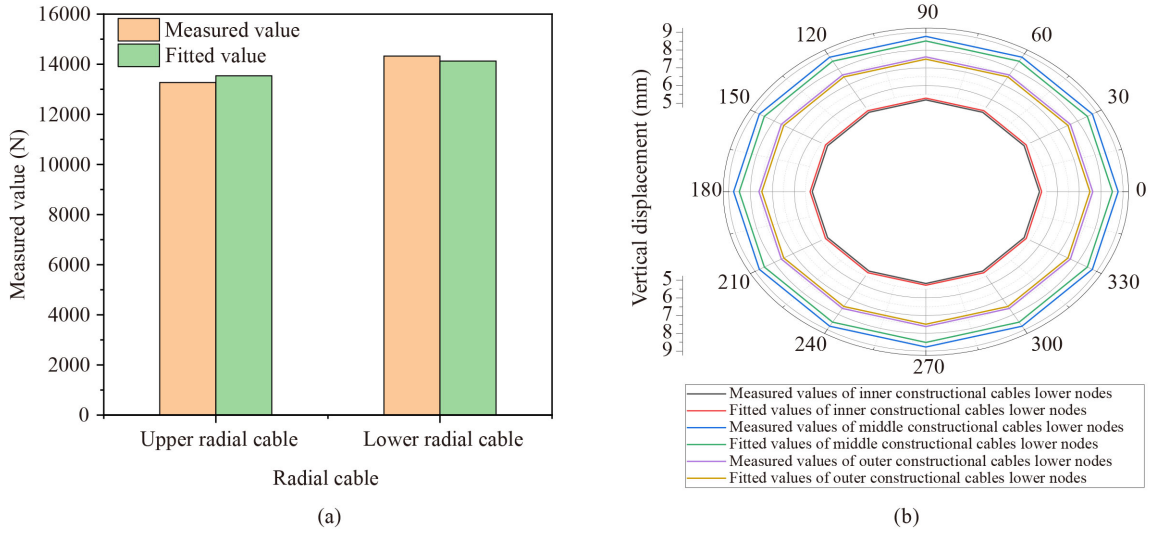

Fig. 18 Comparison between fitted and measured values of MPs: (a) cable force comparison; (b) node displacement comparison.

MPs, the structural safety requirements were satisfied. The values of the MPs were also discretized on the interval (Table 3) to facilitate the safety classification. The influence degree of various DPs on each MP was assessed. The key DPs affecting the MPs were identified, and the relationships between the key DPs and the MPs were revealed. By establishing the functional relationship between MPs and key DPs, the dimension of calculation was effectively reduced. In accordance with the principle of optimal selection, the most suitable structural model was selected by considering the safety performance associated with the structure's MPs, alongside the cost factors tied to the DPs. On the fixed premise of ensuring the safety of the structure, the material consumption was reduced by more than 20%.

The parameter optimization method proposed in this study was verified in the experimental cable truss structure, which can provide a reference for the design of string structures, cable domes and other prestressed steel structures. However, for the design of other types of structures such as frame structures and fabricated structures, it is necessary to further obtain key DPs and analyze mechanical properties. In addition, this study extracted a large number of data samples when establishing a neural network. In the future, structural mechanics performance analysis methods based on small sample data should also be studied.

8 Conclusions and prospects

The conventional approach to structural design has been deficient in including comprehensive consideration of safety, cost, and other pertinent factors. Given the myriad parameter variables inherent in prestressed steel structure design, the traditional method may fall short in addressing the complexities of multi-variable optimization. Addressing this, the current study has introduced a method to optimize DPs for prestressed steel structures, driven by the intricate interplay of multiple factors. Grounded in the associations between DPs and MPs, an intelligent framework, encompassing data association, parameter analysis, and optimization selection for prestressed steel structures, has been formulated. Ultimately, the optimal DPs were assessed through the modeling of structural parameter relationships and the scrutiny of mechanical characteristics. This theoretical approach stands as a guiding reference for the practical engineering design. Throughout the course of this research, the following primary conclusions were drawn.

1) Within the framework of the BP neural network, the inherent design attributes of prestressed steel structures were amalgamated, culminating in the establishment of a robust correlation model for structural parameters. This model enabled the extraction of MPs as outputs based on DPs. This interplay of parameters and the intricate relationship between them provided the basis for the analysis of mechanical performance and the subsequent optimization selection of the structure.

2) Building upon the foundation of the parameter correlation relationships, a systematic classification of MPs was undertaken employing the Random Forest algorithm. This meticulous approach yielded a refined and precise mechanical performance analysis model. Within this model, the validity of structural design feasibility assessment was bolstered, affording the identification of pivotal DPs governing the fluctuations in diverse MPs. The resulting intricate mapping relationship forged between key DPs and MPs effectively mitigated the computational burden associated with structural design. Moreover, the ensuing comprehension of the structure's mechanical attributes provided a basis for ensuring the safety and upkeep of the structure throughout its construction, operational, and maintenance phases.

3) Leveraging the interplay between DPs and MPs, an inclusive evaluation including cost factors and safety considerations was carried out. The pursuit of the optimal structural design, guided by the GA, culminated in a solution that strikingly curtailed material expenses without compromising essential structural integrity.

4) The optimization methodology for DPs in prestressed steel structures was practically applied within the gymnasium design context, including measurements of a physical model, thereby corroborating the method's viability. The efficiency gains were striking, with the design timeline shrinking by over 90% and material usage demonstrating a commendable reduction of more than 20%. Empirical validation underscored the correlation's precision in mechanical property analysis, effectively mitigating reliance on physical test outcomes.

This study has advanced the intelligence of prestressed steel structure design, facilitating the exchange of information across design, construction, and operation stages. As the structural optimization process unfolds, the weighting of diverse parameters also warrants examination, constituting a key aspect of forthcoming research. Future endeavors could explore shared mechanisms within intelligent optimization strategies, fostering enhanced technological research and application.

Acknowledgements The authors gratefully acknowledge the financial support provided by the National Natural Science Foundation of China (Grant No. 5217082614).

Competing interests The authors declare that they have no competing interests.

References

1. Krishnan S. Structural design and behavior of prestressed cable

domes. Engineering Structures, 2020, 209: 110294
2. Ahmed E A, Nassef A O, El Damatty A A. NURBS-based form-finding algorithm for double-curvature cable domes. Engineering Structures, 2023, 283: 115877
3. Zhu Z Y, Bai G B, Zhou Z F. Force finding of cable structures based on singular value decomposition of expanded generalized equilibrium matrix. Journal of Building Structures, 2023, 44(4): 118–128 (in Chinese)
4. Chen L M, Gao W F, Jiang Z C, Zhang H, Liu Y, Zhou Y Y, Dong S L. Section optimization design of a cable dome structure based on robustness. Journal of Building Structures, 2021, 42(7): 104–108 (in Chinese)
5. Knawa-Hawryszków M. Determining initial tension of carrying cable in nonlinear analysis of bi-cable ropeway—Case study. Engineering Structures, 2021, 244: 112769
6. Zhao L, Cao Z, Wang Z, Fan F. Initial prestress design and optimization of cable-stiffened latticed shells. Journal of Constructional Steel Research, 2021, 184(2): 106759
7. Chen L M, Dong S L. Optimal prestress design and construction technique of cable-strut tension structures with multi-overall selfstress modes. Advances in Structural Engineering, 2013, 16(10): 1633–1644
8. Lee S, Lee J. A novel method for topology design for tensegrity structures. Composite Structures, 2016, 152(15): 11–19
9. Huang W, Pei M, Liu X, Wei Y. Design and construction of super-long span bridges in China: Review and future perspectives. Frontiers of Structural and Civil Engineering, 2020, 14(4): 803–838
10. Shishegaran A, Karami B, Danalou E S, Varaee H, Rabczuk T. Computational predictions for predicting the performance of steel 1 panel shear wall under explosive loads. Engineering Computations, 2021, 38(9): 3564–3589
11. Wang L X, Liu H B, Chen Z H, Zhang F, Guo L. Combined digital twin and hierarchical deep learning approach for intelligent damage identification in cable dome structure. Engineering Structures, 2023, 274: 115172
12. Mokhtari F, Imanpour A. A digital twin-based framework for multi-element seismic hybrid simulation of structures. Mechanical Systems and Signal Processing, 2023, 186: 109909
13. LeCun Y, Bengio Y, Hinton G E. Deep learning. Nature, 2015, 521(7553): 436–444
14. Es-Haghi M S, Shishegaran A, Rabczuk T. Evaluation of a novel asymmetric genetic algorithm to optimize the structural design of 3D regular and irregular steel frames. Frontiers of Structural and Civil Engineering, 2020, 14(5): 1110–1130
15. Shishegaran A, Khalili M R, Karami B, Rabczuk T, Shishegaran A. Computational predictions for estimating the maximum deflection of reinforced concrete panels subjected to the blast load. International Journal of Impact Engineering, 2020, 139: 103527
16. Ma G, Liu K. Prediction of compressive strength of CFRP-confined concrete columns based on bp neural network. Journal of Hunan University (Natural Sciences), 2021, 48(9): 88–97 (in Chinese)
17. Zhao Y N, Du W F, Wang Y Q, Wang H, Zhao B Q, Dong S L. Study on intelligent shape finding for tree-like structures based on BP neural network algorithmi. Journal of Building Structures, 2022, 43(4): 77–85 (in Chinese)
18. Shishegaran A, Varaee H, Rabczuk T, Shishegaran G. High correlated variables creator machine: Prediction of the compressive strength of concrete. Computers and Structures, 2021, 247: 106479
19. Chen K, Huang H W, Zhang D M, Zhai W Z, Zhang D M. Constrained multi-objective optimization algorithm based design method of shield tunnel. China Civil Engineering Journal, 2020, 53(S1): 81–86 (in Chinese)
20. Vo-Duy T, Duong-Gia D, Ho-Huu V, Vu-Do H C, Nguyen-Thoi T. Multi-objective optimization of laminated composite beam structures using NSGA-II algorithm. Composite Structures, 2017, 168: 498–509
21. Naghsh M A, Shishegaran A, Karami B, Rabczuk T, Shishegaran A, Taghavizadeh H, Moradi M. An innovative model for predicting the displacement and rotation of column-tree moment connection under fire. Frontiers of Structural and Civil Engineering, 2021, 15(1): 194–212
22. Karami B, Shishegaran A, Taghavizade H, Rabczuk T. Presenting innovative ensemble model for prediction of the load carrying capacity of composite castellated steel beam under fire. Structures, 2021, 33: 4031–4052
23. Shishegaran A, Saeedi M, Mirvalad S, Korayem A H. Computational predictions for estimating the performance of flexural and compressive strength of epoxy resin-based artificial stones. Engineering with Computers, 2023, 39(1): 347–372
24. Bigdeli A, Shishegaran A, Naghsh M A, Karami B, Shishegaran A, Alizadeh G. Surrogate models for the prediction of damage in reinforced concrete tunnels under internal water pressure. Journal of Zhejiang University-Science A, 2021, 22(8): 632–656
25. Liu Z, Jiang A, Shao W, Zhang A, Du X. Artificial-neural-network-based mechanical simulation prediction method for wheel-spoke cable truss construction. International Journal of Steel Structures, 2021, 21(3): 1032–1052
26. Cao T, D'Acunto P, Castellón J J, Tellini A, Schwartz J, Zhang H. Design of prestressed gridshells as smooth poly-hypar surface structures. Structures, 2021, 30(4): 973–984
27. Quagliaroli M, Malerba P G, Albertin A, Pollini N. The role of prestress and its optimization in cable domes design. Computers and Structures, 2015, 161: 17–30
28. Marbaniang A L, Dutta S, Ghosh S. Updated weight method: An optimisation-based form-finding method of tensile membrane structures. Structural and Multidisciplinary Optimization, 2022, 65(6): 169
29. Soltoggio A, Stanley K O, Risi S. Born to learn: The inspiration, progress, and future of evolved plastic artificial neural networks. Neural Networks, 2018, 108: 48–67
30. Hsiao C H, Chen A Y, Ge L, Yeh F. Performance of artificial neural network and convolutional neural network on slope failure prediction using data from the random finite element method. Acta Geotechnica, 2022, 17(12): 5801–5811
31. Afram A, Janabi-Sharifi F, Fung A S, Raahemifar K. Artificial neural network (ANN) based model predictive control (MPC) and optimization of HVAC systems: A state of the art review and case study of a residential HVAC system. Energy and Building, 2017, 141(4): 96–113
32. Li B, Zhuang X. Multiscale computation on feedforward neural

network and recurrent neural network. Frontiers of Structural and Civil Engineering, 2020, 14(6): 1285–1298
33. Ji X, Yang B, Tang Q. Acoustic seabed classification based on multibeam echosounder backscatter data using the PSO-BP-AdaBoost algorithm: A case study from Jiaozhou Bay, China. IEEE Journal of Oceanic Engineering, 2020, 46(2): 509–519
34. Parisi G I, Kemker R, Part J L, Kanan C, Wermter S. Continual lifelong learning with neural networks: A review. Neural Networks, 2019, 113: 54–71
35. Lachhwani K. Application of neural network models for mathematical programming problems: A state of art review. Archives of Computational Methods in Engineering, 2020, 27(1): 171–182
36. Yang H, Li X, Qiang W, Zhao Y, Zhang W, Tang C. A network traffic forecasting method based on SA optimized ARIMA-BP neural network. Computer Networks, 2021, 193(3): 108102
37. Liu G R. The smoothed finite element method (S-FEM): A framework for the design of numerical models for desired solutions. Frontiers of Structural and Civil Engineering, 2019, 13(2): 456–477
38. Liu Z S, Li H, Liu Y, Wang J C, Tafsirojjaman T, Shi G. A novel numerical approach and experimental study to evaluate the effect of component failure on spoke-wheel cable structure. Journal of Building Engineering, 2022, 61: 105268
39. Ding M, Luo B, Han L, Shi Q, Guo Z. Optimal design of spoke double-layer cable-net structures based on an energy principle. Structural Engineering and Mechanics, 2020, 74(4): 533–545
40. Wang B, Gao L, Juan Z. Travel mode detection using GPS data and socioeconomic attributes based on a random forest classifier. IEEE Transactions on Intelligent Transportation Systems, 2018, 19(5): 1547–1558
41. Tan J, Xie X, Zuo J, Xing X, Liu B, Xia Q, Zhang Y. Coupling random forest and inverse distance weighting to generate climate surfaces of precipitation and temperature with multiple-covariates. Journal of Hydrology, 2021, 598(7): 126270
42. Talaslioglu T. Optimal design of steel skeletal structures using the enhanced genetic algorithm methodology. Frontiers of Structural and Civil Engineering, 2019, 13(4): 863–889
43. JGJ 257-2012. Technical Specification for Cable Structures. Beijing: China Architecture & Building Press, 2012 (in Chinese)
44. ASCE/SEI 19-10. Structural Applications of Steel Cables for Buildings. Reston, VA: ASCE, 2010
45. Wang Y L, Wu Z P, Guan G, Li K, Chai S H. Research on intelligent design method of ship multi-deck compartment layout based on improved taboo search genetic algorithm. Ocean Engineering, 2021, 225(2): 108823
46. ANSYS. ANSYS User's Manual Release 15, Swanson Analysis Systems Houston, 2013
47. Kim M K, Kim Y S, Srebric J. Impact of correlation of plug load data, occupancy rates and local weather conditions on electricity consumption in a building using four back-propagation neural network models. Sustainable Cities and Society, 2020, 62: 102321
48. Kaveh A, Rezaei M. Optimum topology design of geometrically nonlinear suspended domes using ECBO. Structural Engineering and Mechanics, 2015, 56(4): 667–694
49. Zhang Q, Zhang Y, Yao L, Fan F, Shen S. Finite element analysis of the static properties and stability of a 800 m Kiewitt type mega-latticed structure. Journal of Constructional Steel Research, 2017, 137: 201–210
50. GB 50009-2012. Load Code for the Design of Building Structures. Beijing: China Architecture & Building Press, 2012 (in Chinese)
51. Samaniegoc E, Anitescud C, Goswamid S, Nguyen-Thanhe V M, Guoe H, Hamdiae K, Zhuange X, Rabczuk T. An energy approach to the solution of partial differential equations in computational mechanics via machine learning: Concepts, implementation and applications. Computer Methods in Applied Mechanics and Engineering, 2020, 362: 112790